Concurrent assessment of motor unit firing properties and fascicle length changes with high-density surface electromyography ultrasound-transparent electrodes

Eduardo Martinez-Valdes[1], *Francesco Negro[2], Alberto Botter[3,4], Giacinto Luigi Cerone[3,4], Deborah Falla[1], *Patricio A Pincheira[4], Glen A Lichtwark[5], Andrew G Cresswell[5]

[1] Centre of Precision Rehabilitation for Spinal Pain, School of Sport, Exercise and Rehabilitation Sciences, University of Birmingham, United Kingdom.

[2] Department of Clinical and Experimental Sciences, Universita` degli Studi di Brescia, Brescia, Italy.

[3] Laboratory for Engineering of the Neuromuscular System (LISiN), Department of Electronics and Telecommunication, Politecnico di Torino, Torino, Italy.

[4] PoliToBIOMed Lab, Politecnico di Torino, Turin, Italy.

[5]School of Human Movement and Nutrition Sciences, The University of Queensland, Australia

*Authors contributed equally

Corresponding Author:

Eduardo Martinez-Valdes

Centre of Precision Rehabilitation for Spinal Pain, School of Sport, Exercise and Rehabilitation Sciences, University of Birmingham, United Kingdom.

Edgbaston B15 2TT

e.a.martinezvaldes@bham.ac.uk

+44 0 121 4158187

KEY POINTS

- We used ultrasound-transparent high-density surface EMG (HDEMG-US) electrodes to examine motor unit firing properties and how this relates to changes in fascicle length, a novel method to better understand the interplay between neural activity and muscle mechanics
- For the first time, we showed that it is possible to identify multiple tibialis anterior motor units with HDEMG-US electrodes, revealing close relationships between fluctuations in discharge rate, fascicle length and dorsiflexion torque
- Delays between neural drive and muscle contraction as well as muscle shortening are reduced compared to the external torque, making this methodology more suitable for understanding motor unit recruitment strategies

ABSTRACT

Previous studies assessing relationships between muscle mechanics and neural activity have concurrently assessed changes in fascicle length (FL) and neural activation with electromyography (EMG) with low spatial sampling from different muscle regions. We used a new ultrasound-transparent high-density EMG electrode (HDEMG-US) to assess changes in FL and motor unit (MU) firing, simultaneously, on the same region of interest. EMG signals and ultrasound images were recorded simultaneously from the tibialis anterior muscle, using a silicon matrix of 32 electrodes, while performing sustained and torque-varying isometric ankle-dorsiflexion contractions, at diverse joint positions (0˚ and 30˚ plantar flexion) and torques (20% and 40% of maximum (MVC)). EMG signals were decomposed into individual MUs and changes in FL were assessed with a fascicle-tracking algorithm. MU firing data was converted into a cumulative spike train (CST) that was cross-correlated with dorsiflexion torque (CST-torque) and FL (CST-FL). On average, 7 (3) MUs were identified across contractions. Cross-correlations showed that CST could explain 60% (range: 31-85%) and 71% (range: 31-88%) of the variance in FL and torque, respectively. Cross-correlation lags revealed that the delay between CST-FL (~75ms) was considerably smaller than CST-torque (~150ms, $p<0.001$). These delays affected the interpretation of MU recruitment/de-recruitment thresholds, with FL showing consistent lengths for both recruitment and de-recruitment. This study is the first to demonstrate the feasibility of recording single-MU activity with HDEMG-US whilst simultaneously evaluating changes in FL, which provides new opportunities for more complex examinations of the interplay between fascicle dynamics and motor unit discharge rates under different contraction conditions.

INTRODUCTION

One of the most fundamental issues in motor control is to understand how the nervous system interacts with muscles for the generation and control of movement. While some answers have been obtained from separate studies in the fields of neurophysiology and biomechanics, there has been a failure to effectively integrate these two disciplines in order to provide clearer information on how neural activity is influenced by muscle mechanics and vice-versa (Enoka, 2004; Tytell *et al.*, 2011). The integration of electromyography (EMG) recordings and ultrasound imaging has given important information about both the mechanisms of muscle activation and contraction, respectively (Hodges *et al.*, 2003; Brown & McGill, 2010; Barber *et al.*, 2013; Day *et al.*, 2013; Pincheira *et al.*, 2018). These techniques helped to determine the level of muscle activity related with a given change in fascicle length and allowed the establishment of relationships between active/passive tissue mechanics (i.e., muscle and tendon compliance) and muscle activity. However, there are many limitations to current approaches at linking muscle mechanics with neural drive to muscles. For example, numerous studies have employed amplitude estimates from bipolar surface EMG recordings in order to assess changes in neural activity and the resultant force produced by muscles (Heintz & Gutierrez-Farewik, 2007; Son *et al.*, 2010; Yoshitake & Shinohara, 2013; Suzuki *et al.*, 2021). Due to many factors such as crosstalk, amplitude cancellation and underlying changes in muscle length and velocity, surface EMG amplitude is unfortunately poorly correlated with the resultant force produced by muscles and therefore cannot be used to directly understand the neural determinants of muscle contractions (Negro *et al.*, 2009; Dideriksen *et al.*, 2018; Dideriksen & Farina, 2019). Furthermore, studies that have examined changes in muscle architecture directly using ultrasound (Hodges *et al.*, 2003; Day

92 *et al.*, 2013; Begovic *et al.*, 2014; Ling *et al.*, 2020) do not image from the same region as the EMG
93 is collected (Vieira & Botter, 2021). Therefore, changes in muscle architecture and/or
94 morphology from different regions could potentially provide results that are not related from
95 those studied on the region of interest. Finally, few studies have also used fine wire
96 electromyography with ultrasound imaging to assess motor unit behaviour in relation to
97 contraction dynamics (Pasquet *et al.*, 2005, 2006; Lauber *et al.*, 2014), however, due to its high
98 selectivity, this technique can only sample a small muscle region, which results in relatively low
99 samples of individual motor units (Farina *et al.*, 2016), reducing the ability to correlate neural
100 drive received by muscles to the mechanical output.
101 Ultrasound translucent high-density EMG (HDEMG-US) electrodes have been developed to
102 enable emerging techniques to sample larger numbers of motor units during muscle contractions
103 (Botter *et al.*, 2013). This approach allows simultaneous recording of high-density EMG with
104 ultrasound images sampled from the same region of interest. The technique has the potential to
105 improve our understanding of the neuromechanical determinants of movement, however to-
106 date this method has not been used to relate single motor unit discharge characteristics (e.g.
107 blind-source separation decomposition) with dynamic fascicle movement tracked from the
108 ultrasound images.
109 Our primary aim was to develop a method to assess motor unit firing characteristics in relation
110 to muscle fascicle dynamics during force development and sustained isometric contraction. To
111 demonstrate the efficacy of using fascicle length changes to understand modulations in motor
112 unit discharge properties, we examined the relationship between motor unit cumulative spike
113 train (CST) and both fascicle length changes and dorsiflexion torque output of the tibialis anterior

muscle. Because the fascicle shortening during isometric contraction is related to force output (due to stretch of the in-series tendon), we expect the correlation between CST and fascicle shortening will be similar to that between CST and torque, but with a reduced lag due to the faster conversion of motor unit activity into contraction (compared to the conversion of motor unit activity into torque). We also examined differences in recruitment threshold when considered in terms of fascicle length or torque, as possible delays between these signals, might affect the interpretation of motor unit recruitment and de-recruitment thresholds.

METHODS

The study was conducted at the school of Human Movement and Nutrition Sciences of the University of Queensland, Australia. All procedures were approved by the University of Queensland ethical committee (approval number: 2019001675) and were conducted in accordance with the Declaration of Helsinki. Ten healthy young male volunteers participated [age: mean (SD) 29 (5) years]. Exclusion criteria included any neuromuscular disorder, musculoskeletal injuries such as muscle strain as well as any current or previous history of lower limb pain/injury and age <18 or >35 years. Participants were asked to avoid any strenuous activity 24 h before the measurements.

Task

Participants were seated in a reclined position on the chair of an isokinetic dynamometer (Humac Norm, CSMi Computer Sports Medicine, Stoughton, USA). The right leg (dominant for all participants) was extended and positioned over a support with the knee flexed to 10° (with 0° representing full knee extension). The centre of rotation of the ankle joint (lateral malleoli) was

aligned to the centre of rotation of the isokinetic dynamometer in order to accurately quantify ankle dorsi-flexion torque. Participants performed sustained and torque-varying isometric dorsiflexion contractions at different torque levels at short (ankle at 0° plantar flexion) and long muscle lengths (ankle at 30° plantar flexion). A study schematic describing the measurements performed during the session can be seen in **Figure 1**. The session began with the participants' performing three isometric ankle dorsiflexion maximum voluntary contractions (MVC) at each ankle angle, where each MVC was separated by 2-min of rest. The order in which the ankle was positioned (short and long tibialis anterior lengths) was randomized. Following the MVC assessment, participants were allowed to practice with visual feedback of their exerted torque (displayed on a computer monitor), by performing brief ramp-hold contractions at low torque levels (20% MVC). Then, after 5 min of rest, participants performed ramp-hold (sustained) and torque-varying sinusoidal contractions at 20% or 40% MVC. For sustained isometric contractions, participants were asked to increase their torque at a rate of 10% MVC/s and then to hold the contraction at the target level for 30 s, therefore reaching the 20% MVC target in 2 s and the 40% MVC in 4 s. Two sustained 20% MVC and two sustained 40% MVC contractions were performed. For the torque-varying sinusoidal isometric contractions, the participants reached an average torque target of 20 and 40% MVC, at a frequency of 0.5 Hz and amplitude modulation of 5% MVC. One sinusoidal contraction per torque level was performed. These sinusoidal contractions aimed to test the ability of both the motor unit decomposition and fascicle tracking algorithms to identify motor units and track changes in fascicle length in conditions where the variability of motor unit firing and fascicle length is increased. All these isometric contractions were executed

in a randomized order across participants at each muscle length, but the order of the randomization was kept constant between 0˚ and 30˚ of plantar flexion.

Electromyography

Surface EMG signals were recorded from the tibialis anterior muscle using a high-density, 32-channel, HDEMG-US electrode grid (LiSIN, Torino, Italy) (Botter *et al.*, 2013). Each grid consists of 8 x 4 electrodes (1-mm diameter, 10-mm interelectrode distance in both directions) embedded into a layer of silicon rubber (**Figure 2A)**. The array was located centrally between the proximal and distal tendons of the muscle, with the columns oriented parallel to the tibia bone (Martinez-Valdes *et al.*, 2020b). Skin-electrode contact was made by inserting conductive gel (Sonogel, Bad Camberg, Germany) into the electrode cavities with a mechanical pipette (Eppendorf, Hamburg, Germany) as seen previously (Botter *et al.*, 2013). Signals were amplified and recorded using a new wireless wearable HDEMG amplifier (Cerone *et al.*, 2019) (**Figure 2B),** directly connected to the grid of electrodes, which is ideal when HDEMG measurements are combined with other methods such as ultrasound imaging. The amplifier was light and compact (16.7 g and 3.4 cm x 3 cm x 1.5 cm), and contained a 16-bit analogue-digital converter. For this experiment, data was recorded in monopolar mode at a sampling frequency of 2048 Hz, with a gain of 192 ± 1 V/V and a band-pass filter with cut-off frequencies between 10-500 Hz. Torque data was also sampled at 2048Hz and recorded through the auxiliary input of the HDEMG amplifier. All EMG and torque data were processed and analysed offline using MATLAB 2019b (MathWorks Inc., Natick, MA).

Ultrasonography

Ultrasound images of tibialis anterior fascicles were captured using B-mode ultrasonography (6 MHz, 80 frames per second, 60 mm field of view) using a 128-element multi-frequency

transducer (LF9-5N60-A3; Telemed, Vilnius, Lithuania) attached to a PC-based ultrasound system (ArtUs EXT-1H scanner; Telemed, Vilnius, Lithuania). A dry HDEMG-US grid (without conductive gel) was first used to find the best alignment of the probe allowing clear visualization of the muscle's fascicles when the probe is placed over the electrodes. Once the optimal position was identified, the skin was marked with an indelible pen. Then, the HDEMG-US electrode grid electrode cavities were filled with conductive gel and positioned over the tibialis anterior muscle. The flat-shaped ultrasound transducer was then placed over the electrode grid and firmly strapped over the leg using an elastic bandage to prevent any movement. An example of the setup and an ultrasound image can be seen in **Figure 2B.**

HDEMG and ultrasound synchronization

Torque, position, HDEMG, and ultrasound data were synchronized utilising an analogue pulse sent from an AD board (Micro 1401-3, Cambridge Electronic Design, Cambridge, UK). The trigger signal was set at 80 Hz and controlled frame by frame the ultrasound recording (i.e. every time the beamformer received a pulse, one frame of ultrasound data was recorded). The same trigger signal was sent to the auxiliary input of the HDEMG device and was aligned offline with the tracked fascicle data (see next section) obtained from the ultrasound files.

Motor unit decomposition and fascicle length tracking

The HDEMG signals were decomposed into motor unit spike trains with an extensively validated blind source separation algorithm, which provides automatic identification of the activity of multiple single motor units (Negro *et al.*, 2016). Each identified motor unit was assessed for decomposition accuracy with a validated metric (Silhouette, SIL), which represents the sensitivity of the decomposed spike train. Since the identification of motor unit activity with HDEMG-US

grids is more challenging due to the lower selectivity of these grids (i.e., 32 channels and inter-electrode distance of 10 mm), an accuracy level of 0.86 SIL (86% of accuracy) was used to approve or discard any motor unit (usual threshold is set at 0.90 SIL (Negro *et al.*, 2016; Martinez-Valdes *et al.*, 2020a). Moreover, further examination of each spike train was performed, and all firings separated from the next by <33.3 ms or >200 ms were re-checked manually by an experienced operator E.M.-V. (Afsharipour *et al.*, 2020; Cogliati *et al.*, 2020) and the motor unit pulse trains were re-computed. After this procedure, the average SIL value increased to 0.90 (0.007).

Tibialis anterior fascicle length changes were tracked offline by employing custom-made software (Farris & Lichtwark, 2016) utilizing a previously validated Lucas-Kanade optical flow algorithm with affine transformation (Gillett *et al.*, 2013; Farris & Lichtwark, 2016). From each trial, we selected the fascicle in which we were able to visualize ~80% of its length within the field of view of the image. We selected a fascicle from the anterior compartment of the tibialis anterior muscle because 1) this was the region of motor unit activity that was likely covered by the HDEMG electrode and 2) our preliminary results showed that changes in fascicle length from this region are enough to explain at least 70% of the variance in the resultant torque output (see results). Changes in fascicle length were analysed according to shortening length [Δ fascicle length (i.e. difference in fascicle length from rest to target torque (20% MVC)], in order to 1) understand the amount of fascicle shortening required to recruit a motor unit and reach the required torque level (20% MVC and 40% MVC), and 2) to be able to correlate fluctuations in fascicle length with fluctuations in motor unit discharge rate, since absolute changes in fascicle length go in an opposite direction to discharge rate (fascicle length decreases when discharge rate increases, see next section). We also estimated pennation angle as the angle between the

fascicle and its insertion into the central aponeurosis (Reeves & Narici, 2003). The pennation angle was calculated when the muscle was at rest and when the torque was stable during the isometric contractions.

Concurrent motor unit and fascicle length analysis

For sustained isometric contractions, mean discharge rate was calculated from the stable plateau torque region. Motor unit recruitment and de-recruitment thresholds were defined as the ankle dorsiflexion torques (%MVC) or fascicle shortening lengths (Δfascicle length, mm) at the times when the motor units began and stopped discharging action potentials, respectively. For these contractions we also tested the possibility to track the same motor units across the two different target torques and muscle lengths, with a previously proposed method based on cross-correlation of 2D motor unit action potentials (MUAPs) (Martinez-Valdes *et al.*, 2017b). In this procedure, MUAP matches between the two correlated trials (i.e. 20% MVC-0˚ vs 20% MVC-30˚) were visually inspected and the two identified motor units were regarded as the same when they had a cross-correlation coefficient >0.80 (Martinez-Valdes *et al.*, 2017b). Cross-correlation (time domain) analysis was also used to assess the interplay between torque, fascicle length and motor unit firing data. For this purpose, motor unit discharge times were summed to generate a cumulative spike train (CST) as done previously (Thompson *et al.*, 2018). Fascicle length signals were interpolated to 2048Hz to match both motor unit and torque data. After these procedures, the CST, fascicle length and torque signals were low-pass filtered (4th order zero-phase Butterworth, 2Hz) and then high-pass filtered (4th order zero-phase Butterworth, 0.75Hz) as presented previously (De Luca & Erim, 1994). These filtered signals were then cross-correlated to assess similarities in their fluctuations (cross-correlation coefficient) and to calculate the lags

between CST vs torque, CST vs fascicle length and fascicle length vs torque. These assessments provided information on the delays generated between the neural drive and torque output, neural drive and muscle contraction and, muscle contraction and torque output.

Statistical Analysis

Results are expressed as mean and (SD). Normality of the data was assessed with the Shapiro-Wilk test and Sphericity was tested with the Mauchly test. Differences between fascicle parameters (absolute changes in length and pennation angle) at short and long muscle lengths during rest were assessed with paired t-tests. Absolute differences in fascicle length and pennation angle during isometric contractions were assessed with a two-way repeated measures ANOVA, with factors of muscle length (0˚ or 30˚ of plantar flexion) and torque (20 or 40% MVC). For motor unit/Δfascicle length data during isometric contractions the following statistical tests were employed: 1) two-way repeated measures ANOVA with factors of muscle length and torque to assess differences in discharge rate 2) three-way repeated measures ANOVA with factors of muscle length, torque and signal comparison (CST vs torque, fascicle length vs CST, and torque vs fascicle length) to assess differences in cross-correlation results (correlation coefficient and lag) 3) three-way repeated measures analysis of variance (ANOVA) with factors of muscle length, torque and recruitment (recruitment vs de-recruitment) to assess differences between recruitment and de-recruitment thresholds (in terms of %MVC torque and Δfascicle length). Finally, all cross-correlation results obtained during sustained and sinusoidal contractions were averaged for each contraction type and compared by paired t-test. All ANOVA analyses were performed on STATISTICA 12 (Statsoft, Tulsa, USA) and followed by pairwise comparisons with a

Student-Newman-Keuls (SNK) post hoc test when significant. Statistical significance was set at $p<0.05$.

RESULTS

Maximal torque, motor unit decomposition and tracking during isometric contractions

The MVC dorsiflexion torque differed at the two ankle positions and was 25.2 (13.2) and 51.8 (12.5) Nm at short (0° plantarflexion) and long (30° plantarflexion) muscle lengths, respectively ($p<0.001$). During both sustained and sinusoidal isometric contractions, an average of 7 (3), 7 (2), 7 (3) and 6 (2) motor units could be identified per participant at 20% MVC-0˚, 20% MVC-30˚, 40% MVC-0˚ and 40% MVC-30˚, respectively. A representative example with the decomposition results from one participant can be seen in **Figure 3.** In this particular example, each motor unit has a clearly distinct MUAP shape (right side of the figure) which allowed accurate identification of discharge times (left side of the figure). An average of 3 (2) motor units could be tracked successfully per participant across the two muscle lengths [2D MUAP cross-correlation coefficient 0.83 (0.03)] and 3 (1) motor units per participant across the two torque levels [2D MUAP cross-correlation coefficient 0.88 (0.05)]. A representative example of the tracking procedure across the two joint angles with the HDEMG-US grids can be seen in **Figure 4**.

Relationships between fascicle length, torque and motor unit discharge rate during isometric contractions

Absolute fascicle lengths and pennation angles during rest and isometric contractions at the different torque targets and joint angles are presented in **Table 1.** Overall, tibialis anterior fascicles were longer and had smaller pennation angles at 30˚ of plantar flexion at rest and during contractions ($p<0.001$). Nevertheless, fascicle lengths decreased (torque effect: $p<0.001$,

η^2=0.78) and pennation angles increased (torque effect: p=0.018, η^2=0.48) similarly with increasing torque at both 0˚ and 30˚ of plantarflexion.

Table 1. Fascicle length and pennation angles at rest and during sustained isometric contractions at 20% and 40% MVC at short and long muscle lengths

	Short (0˚plantar flexion)	Long (30˚ plantar flexion)	P-value
Pennation angle (°), rest	15.2 (1.7)	12.0 (1.7)	<0.001
Fascicle length (mm), rest	60.2 (8.8)	74.5 (9.1)	<0.001
Pennation angle (°), 20% MVC	19.2 (3.7)	16.9 (3.9)	0.001#
Fascicle length (mm), 20% MVC	52.7 (7.5)	66.3 (9.4)	<0.001*
Pennation angle (°), 40% MVC	20.8 (3.1)	17.4 (4.0)	0.001#
Fascicle length (mm), 40% MVC	50.8 (6.9)	61.9 (7.9)	<0.001*

*Significant effect of torque (p<0.001)
#Significant effect of torque (p=0.018)

Similar to the changes in fascicle length, the tracking of individual motor units across short and long muscle lengths revealed similar discharge rates at the different joint angles (15.3 (2.6) Hz and 14.7 (1.4) Hz at 20% MVC, and 16.7 (2.3) Hz and 17.0 (2.4) Hz at 40% MVC, between 0˚ and 30˚ of plantar flexion, respectively, muscle length effect: p=0.74, η2=0.047), but increased firing frequency between the different torque levels (torque effect: p=0.03, η^2=0.43). A representative example of the concurrent assessment of changes in fascicle length, torque and CST can be seen in **Figure 5.** Briefly, after the offline identification/tracking of the fascicle (**Figure 5A**), and the identification/editing of the motor unit spike trains and subsequent conversion to CSTs, three signals were obtained: torque, fascicle length and CST. All these signals were then cross-correlated on the stable torque part of the contraction (**Figure 5B**, upper panel) in order to assess common fluctuations between torque, CST and fascicle length signals. All comparisons showed high levels of cross-correlation (CST vs torque, CST vs fascicle length and fascicle vs torque, **Figure**

5B, bottom panel) and the lags obtained, showed the delay between: neural drive and resultant torque output (CST vs torque), neural drive and muscle contraction (CST vs fascicle length) and, muscle contraction and resultant torque output (fascicle length vs torque). The cross-correlation results for the group of participants are presented in **Table 2**. Overall, all cross-correlation coefficients were high as each of the signals could explain on average, at least 50% of the variance in resultant torque, CST and fascicle length, showing that there was a strong relationship between these variables. It is worth noting that all correlation coefficients were higher during the sinusoidal contractions ($p=0.001$, **Table 2**). Nevertheless, the cross-correlation between CST vs fascicle length was significantly smaller compared to the other signal comparisons in both contraction types (signal comparison effect: $p=0.007$, $\eta2=0.427$ and $p<0.0001$, $\eta2=0.846$, for sustained and sinusoidal contractions, respectively). Cross-correlation lags (**Figure 6**) during sustained isometric contractions at 30˚ of plantar flexion were larger than those at 0˚ plantar flexion at both torque levels in all signal comparisons, in both sustained (muscle length effect: $p=0.002$, $\eta2=0.66$) and torque-varying sinusoidal (muscle length effect: $p=0.034$, $\eta2=0.39$) isometric contractions, with no differences between sustained vs sinusoidal isometric lag values.

Table 2. Cross-correlation coefficients for comparisons between cumulative spike train (CST) vs torque, CST vs fascicle length and torque vs fascicle length during isometric contractions.

	Short length 20% MVC	Long Length 20% MVC	Short length 40%MVC	Long length 40% MVC
Steady isometric contractions				
Torque vs CST	0.74 (0.65-0.88)	0.74 (0.62-0.85)	0.74 (0.63-0.85)	0.61 (0.31-0.78)
Fascicle vs CST	0.64 (0.51-0.81)	0.57 (0.31-0.75)	0.63 (0.33-0.85)	0.50 (0.31-0.66)
Torque vs Fascicle	0.71 (0.40-0.88)	0.67 (0.33-0.89)	0.78 (0.33-0.93)	0.72 (0.50-0.91)
Oscillatory isometric contractions				
Torque vs CST	0.78 (0.66-0.89)	0.77 (0.62-0.83)	0.77 (0.66-0.89)	0.66 (0.45-0.82)
Fascicle vs CST	0.71 (0.58-0.86)	0.73 (0.69-0.78)	0.74 (0.60-0.86)	0.62 (0.41-0.75)
Torque vs Fascicle	0.87 (0.75-0.95)	0.89 (0.75-0.95)	0.91 (0.80-0.96)	0.89 (0.77-0.96)

Results are expressed as mean (min-max range).

Variations in fascicle length and recruitment threshold and during isometric contractions

Motor unit recruitment and de-recruitment thresholds in terms of both Δfascicle length (mm) and torque (%MVC) are shown for a representative participant in **Figure 7A**. The figure shows that recruitment threshold torque is higher than the torque at de-recruitment, however, the Δfascicle length at which motor units were recruited and de-recruited was similar. This was confirmed in motor units that were tracked across short and long muscle lengths as de-recruitment thresholds were consistently lower when assessed in terms of %MVC torque (recruitment-de-recruitment effect: $p=0.029$, $\eta^2=0.43$, **Figure 7B**) but similar in terms of Δfascicle length (recruitment-de-recruitment effect $p=0.805$, $\eta^2=0.007$, **Figure 7B**,). In addition, although recruitment and de-recruitment thresholds increased in terms %MVC torque across 20% and 40% MVC levels (torque effect: $p=0.001$, $\eta^2=0.701$), motor units were recruited and de-recruited at a similar Δfascicle length with increasing torque (torque effect: $p=0.731$, $\eta^2=0.014$). Finally,

recruitment-de-recruitment thresholds also increased at long muscle lengths (0° plantar flexion vs 30° plantar flexion) when considered as %MVC torque (muscle length effect: $p<0.001$, $\eta^2=0.77$) but not in terms of Δfascicle length (muscle length effect: $p=0.389$, $\eta^2=0.014$).

DISCUSSION

This is the first study showing simultaneous assessment of motor unit firing properties with changes in fascicle length, on the same region of interest, with HDEMG-US electrodes. Most importantly, these changes could be analysed at different torque levels and over a relatively large range of ankle joint motion (0˚ to 30˚ of plantar flexion). With the combination of these techniques, we identified strong relationships between fluctuations in tibialis anterior discharge rate and fascicle length, as well as fluctuations in fascicle length and the torque produced. These relationships allowed us to quantify the delays between motor unit firing activity and muscle contraction, and muscle contraction and joint torque. As we hypothesised, we were able to show that the delay between CST and fascicle length was smaller than that of CST and torque, which shows that previous measures of electromechanical delay between EMG (Cavanagh & Komi, 1979) or motor unit discharge patterns (Del Vecchio *et al.*, 2018) and force/torque might not provide an adequate estimation of the conversion of neural activity into muscle contraction. In addition, we demonstrated that the delays between the neural drive and fascicle length or the generated force/torque are larger when the muscle contracts isometrically at longer fascicle lengths (**Figure 6**). Finally, due to the possibility to track motor units across different muscle lengths and target torques, we were also able to show that recruitment and de-recruitment thresholds are similar when considered in terms of fascicle length, meaning that motor units are recruited and de-recruited at the same relative fascicle length, regardless of the joint position or

torque exerted. Taken together, the findings of the present study have enhanced our understanding of the interaction between motor unit firing and mechanisms of muscle contraction.

This study is the first to decompose motor unit activity from HDEMG-US grids. The findings showed that an average of 7 motor units could be accurately identified per participant during isometric contractions. The motor units identified with HDEMG-US electrodes had clear distinct MUAP shapes and show differences in activity across different regions of the electrode grid (**Figure 3**). Moreover, by employing the 2D spatial representation of MUAPs we were able to track approximately 40% of the identified motor units across torques and joint angles (**Figure 4**). We previously showed the possibility to track motor units across different force levels with HDEMG, by employing 2D MUAP "signatures" (Martinez-Valdes *et al.*, 2017b). Indeed, the advantage of HDEMG systems is that they show a large spatial representation of MUAPs, which can be used to follow the same units within and across sessions. This methodology has been successfully employed in a number of studies (Martinez-Valdes *et al.*, 2017a; Boccia *et al.*, 2019; Del Vecchio *et al.*, 2019; Murphy *et al.*, 2019). We expanded on that possibility and tracked motor units across different muscle lengths obtaining good results (average correlation of 0.83 between MUAPs). This shows that HDEMG-US electrodes allow the concurrent assessment of changes in motor unit discharge and fascicle length and linking those changes to motor units that can be followed across different joint angles and torque levels, enabling a more reliable assessment of neuromechanical variables.

A number of studies have shown that fluctuations in firing rate are closely related to the fluctuations in torque/force (Negro *et al.*, 2009; Del Vecchio *et al.*, 2018; Thompson *et al.*, 2018).

Considering this observation, we attempted to quantify the level of correlation between fluctuations in firing rate (CST), changes in fascicle length and torque, in order to first, corroborate that the information obtained from the identified motor units was linked to the fascicles of the region of interest (CST vs fascicle length correlation) and also to confirm that motor unit firings identified with HDEMG-US grids would be able to predict the torque produced via the tendon. The findings showed that all of the signals compared had high levels of correlation (CST explained ~70% and ~60% of the variance in torque and fascicle length respectively), confirming that the motor unit data obtained from HDEMG-US grids provided a good representation of the fascicle behaviour of the region of interest. Moreover, all correlation levels increased further when greater torque variability was induced during sinusoidal contractions, which first, confirms the ability of the decomposition algorithm to detect faster changes in motor unit firing and second, shows that the ability of the fascicle tracking algorithm to follow changes in length is improved when more variable isometric contractions are performed. It is important to mention that this greater variability did not affect cross-correlation lags as similar delays were observed in both sustained and oscillatory contractions (**Figure 6**), which shows the robustness of the approach. The lower correlation between CST and fascicle length (**Table 2**) during both sustained and sinusoidal isometric contractions could be explained by a number of factors, including the subtle inaccuracies in fascicle length determination from ultrasound imaging and potential mismatches between fibres contributing to CST and the fibres in the imaging region. It is possible that the fascicle tracking code or the sampling frequency employed to obtain the images (80Hz) was not sensitive enough to detect smaller changes in fascicle length, particularly during sustained contractions. However, the sampling frequency is well above the frequency of

variation in force during isometric contraction (<5Hz (Farina & Negro, 2015)) and tremor (5-13Hz, (Yavuz *et al.*, 2015)). Therefore, it is more likely that limitations in imaging the muscle in a single plane and the resolution of the tracking algorithm may contribute to the lower correlations. The depth at which we tracked the fascicles (superficial portion of the tibialis anterior) vs region of motor units recorded may also contribute to discrepancies in the signal correlations; the HDEMG-US electrodes are most likely to only detect motor unit activity of the most superficial motor units (Farina *et al.*, 2002). If we also consider that blind-source separation motor unit decomposition techniques favour the identification of motor units showing the largest MUAPs and the highest spatial localization on the HDEMG grid (Holobar & Farina, 2014; Negro *et al.*, 2016), it is very likely that the motor units included in the analysis mainly represent the superficial region of tibialis anterior. Nevertheless, it is important to note that our technique provided moderate-high cross-correlations between CST and fascicle length during isometric contractions, which demonstrates feasibility of using such approach to understand the link between motor unit recruitment and muscle mechanics during actual movement.

One of the most interesting findings from this study was the possibility of quantifying delays between CST vs. fascicle length and fascicle length vs. torque. Cross-correlation lags revealed that the time required to shorten the fascicle (conversion of motor unit firings into contraction) was smaller than the time required to produce mechanical output (torque). This finding implies that imaging of the muscle is necessary to determine the time required to convert motor unit discharge activity into contraction. Historically, the conversion of neural activity into mechanical output has usually been assessed by calculating the time-difference between the onset of force/torque and muscle activation (also known as the electromechanical delay (Cavanagh &

Komi, 1979)). This assessment, however, assumes that there is no lag between the generation of a contraction and the transmission of force to the tendon and then transmission to the measuring apparatus. More recent studies that have combined conventional bipolar EMG and ultrasound during voluntary contractions have found that fascicle shortening happen before force/torque is measured (Begovic *et al.*, 2014; Ling *et al.*, 2020), which agrees with our findings. Nevertheless, this assessment has several issues, first, the onset of muscle activation from bipolar EMG signals can be greatly influenced by the electrode's location (Hug *et al.*, 2011), second, fascicle shortening from deeper muscle regions could happen before EMG activity is detected on the surface (Dieterich *et al.*, 2017) and third, the assessment can be confounded by the mechanical impedances of the measuring device (Corcos *et al.*, 1992). Thus, absolute values of electromechanical delay might not provide a reliable assessment of the mechanisms responsible for force generation and transmission (Corcos *et al.*, 1992). For these reasons, we propose that cross-correlation of signals obtained from HDEMG-US motor unit decomposition and ultrasound could provide a better estimation of these delays, as such assessment considers mechanisms responsible for contraction dynamics (i.e. fascicle length responses to firing rate modulations) rather than just assessing delay differences between signals at contraction onset. It is important to mention that our proposed approach shows longer delays in comparison with classical estimations of electromechanical delay (~150ms of delay between CST and torque vs. ~50ms between EMG and torque (Begovic *et al.*, 2014)), possibly due to the time-instant in which these relationships are quantified (contraction onset vs. sustained/torque varying contraction), twitch characteristics of the active motor units (Del Vecchio *et al.*, 2018) and changes in MUAP duration during the contraction. Improved HDEMG decomposition techniques allowing accurate

identification of motor unit activity before contraction onset (which is not currently possible), would allow comparing the delays obtained during force development and sustained contractions, in order to assess potential differences in signal transmission in different phases of isometric contractions.

Another interesting result obtained from the cross-correlation lags was that both CST vs. fascicle length and fascicle length vs. torque delays increased when the muscle contracted isometrically in a lengthened position (**Figure 6**). Changes in the duration of muscle-fibre twitch force and muscle-tendon compliance at larger muscle lengths likely influenced these delays. To provide support to the first observation, several studies have reported that muscle twitches are significantly larger (greater contraction and half-relaxation times) when the muscle is lengthened (Stephens *et al.*, 1975; Marsh *et al.*, 1981; Bigland-Ritchie *et al.*, 1992). Therefore, it is very likely that an increase in the overall duration of the motor unit responses at longer lengths is the reason for the more delayed muscle contraction and transmission of force to the tendon observed at the two submaximal normalized torque targets (20 and 40% MVC). In addition, changes in tendon and aponeurosis elasticity during lengthening could also reduce the amount of neural drive required to activate the muscle (Lichtwark & Wilson, 2007; Mayfield *et al.*, 2016; Raiteri *et al.*, 2018) and potentially increase the delays between signals. Nevertheless, the assessment of both motor unit contractile properties and the effect of passive structural properties of the muscle on motor unit behaviour needs to be confirmed in future investigations. The assessment of these delays holds great potential in both healthy populations (e.g. aging) and patients (e.g. cerebral palsy), as they could help to quantify impairments in force transmission, when muscles have altered architecture (e.g. muscle contractures).

The current methodology presents multiple opportunities to assess interactions between motor unit firing rate/recruitment and changes in fascicle length, however, for this report we wanted to focus on the assessment of recruitment and de-recruitment thresholds in relation to both %MVC torque and fascicle length. We selected these variables because motor unit studies typically use torque to assume changes in muscle behaviour, and delays between motor unit firing and torque due to force transmission delays (along muscle/tendon and also within dynamometer) would create offsets when comparing recruitment (torque rise) vs decruitment (torque drop). The findings from this study in these assessed variables, emphasise the need of quantifying changes in motor unit activity and fascicle length simultaneously. First, we were able to observe that recruitment and de-recruitment thresholds differed when quantified as % MVC torque (recruitment threshold was higher than the de-recruitment threshold) but were similar when quantified in terms of fascicle length. To our knowledge, this is the first study showing this discrepancy. Moreover, we were able to observe that the length at which a motor unit was recruited and de-recruited was maintained across joint angles and torque levels. Fascicle shortening preceded torque generation (as expected), but fascicles returned to resting values after the dorsiflexion torque returned to 0 Nm, meaning that during the ramp-down phase of the contraction, there is a time-point where the muscle returns passively to its original length (**Figure 7**). This can explain why most previous studies show lower torque values for de-recruitment than recruitment when considered as %MVC torque or absolute torque (De Luca, 1985; Romaiguere *et al.*, 1993) and emphasizes the need to quantify these thresholds in terms of fascicle length and not in terms of joint force/torque. Interestingly, similar divergences were recently reported when

considering recruitment and de-recruitment in terms of joint angle or fascicle length during isometric plantarflexion contractions at varying knee-joint angles (Lauber *et al.*, 2014).

Finally, it is worth mentioning that the accurate assessment of motor unit and fascicle data in a variety of contraction types, torque levels and joint positions, opens up the opportunity to explore more dynamic isometric contraction models (i.e., ballistic contractions or faster sinusoidal contractions) and shortening and lengthening contractions. Our present results were not affected by more dynamic variations in isometric torque and the tracking of motor units across joint angles revealed that MUAPs did not change substantially within the range of motion investigated (**Figure 4**). Very recent studies employing HDEMG recordings (without ultrasound) have successfully identified motor units during shortening and lengthening contractions (Glaser & Holobar, 2019; Oliveira & Negro, 2021), therefore, it is very likely that future studies assessing changes in motor unit activity and fascicle length will be able to assess these interactions during dynamic conditions.

In this study we were able identify an average of 7 motor units across contractions, which is lower than the number of units identified with non-transparent HDEMG electrodes, where approximately 15 to 20 motor units can be identified on the tibialis anterior muscle on average per participant (Martinez-Valdes *et al.*, 2020b). These differences can be attributed to a number of factors. First, the grid of electrodes employed in the current study contained 32 electrodes vs. the 64 electrodes conventionally employed to decompose EMG signals. It has been shown that a larger number of channels enhances the spatial identification of MUAPs and therefore improves the separation of the multiple motor unit sources from the HDEMG with blind-source separation methods (Farina *et al.*, 2008; Negro *et al.*, 2016). Second, the inter-electrode distance of the

HDEMG-US grid (10mm) is less selective than the 64-channel grids (8mm) commonly employed to decompose motor unit activity, which can again influence the separation of MUAPs from the HDEMG. Therefore, improvements in electrode construction will likely increase the number of motor units identified with HDEMG-US. Nevertheless, it is important to mention that we were still able to explain ~70% of the of the variance in torque with the number of identified units in the present study, which is similar to the values reported in previous studies (Negro *et al.*, 2009; Del Vecchio *et al.*, 2018; Thompson *et al.*, 2018). Finally, and as mentioned previously, muscle fascicle imaging using ultrasound also has some limitations in terms of the resolution of the image and ability to track length changes, as well as the limitation of only being able to image one plane of the muscle. Improvements in ultrasound probe construction and/or the addition of another ultrasound probe in a different portion of the electrode grid would likely help to improve estimations of changes in fascicle length during isometric contractions.

In conclusion, this study presents, for the first time, the possibility to identify motor units and track changes in fascicle length simultaneously, on the same region of interest, with HDEMG-US electrodes. We showed that this method can be employed over a wide range of conditions, and can provide important information about the inter-relationships between neural drive, fascicle length and torque, which provides new opportunities to assess the neural and mechanical determinants of muscle contractions in both health and disease.

REFERENCES

Afsharipour B, Manzur N, Duchcherer J, Fenrich KF, Thompson CK, Negro F, Quinlan KA, Bennett DJ & Gorassini MA. (2020). Estimation of self-sustained activity produced by persistent inward currents using firing rate profiles of multiple motor units in humans. *J Neurophysiol* **124,** 63-85.

Barber LA, Barrett RS, Gillett JG, Cresswell AG & Lichtwark GA. (2013). Neuromechanical properties of the triceps surae in young and older adults. *Exp Gerontol* **48,** 1147-1155.

Begovic H, Zhou GQ, Li T, Wang Y & Zheng YP. (2014). Detection of the electromechanical delay and its components during voluntary isometric contraction of the quadriceps femoris muscle. *Front Physiol* **5,** 494.

Bigland-Ritchie BR, Furbush FH, Gandevia SC & Thomas CK. (1992). Voluntary discharge frequencies of human motoneurons at different muscle lengths. *Muscle Nerve* **15,** 130-137.

Boccia G, Martinez-Valdes E, Negro F, Rainoldi A & Falla D. (2019). Motor unit discharge rate and the estimated synaptic input to the vasti muscles is higher in open compared with closed kinetic chain exercise. *J Appl Physiol (1985)* **127,** 950-958.

Botter A, Vieira TM, Loram ID, Merletti R & Hodson-Tole EF. (2013). A novel system of electrodes transparent to ultrasound for simultaneous detection of myoelectric activity and B-mode ultrasound images of skeletal muscles. *J Appl Physiol (1985)* **115,** 1203-1214.

Brown SH & McGill SM. (2010). A comparison of ultrasound and electromyography measures of force and activation to examine the mechanics of abdominal wall contraction. *Clin Biomech (Bristol, Avon)* **25,** 115-123.

Cavanagh PR & Komi PV. (1979). Electromechanical delay in human skeletal muscle under concentric and eccentric contractions. *Eur J Appl Physiol Occup Physiol* **42,** 159-163.

Cerone GL, Botter A & Gazzoni M. (2019). A Modular, Smart, and Wearable System for High Density sEMG Detection. *IEEE Trans Biomed Eng* **66,** 3371-3380.

Cogliati M, Cudicio A, Martinez-Valdes E, Tarperi C, Schena F, Orizio C & Negro F. (2020). Half marathon induces changes in central control and peripheral properties of individual motor units in master athletes. *J Electromyogr Kinesiol* **55,** 102472.

Corcos DM, Gottlieb GL, Latash ML, Almeida GL & Agarwal GC. (1992). Electromechanical delay: An experimental artifact. *J Electromyogr Kinesiol* **2,** 59-68.

575 Day JT, Lichtwark GA & Cresswell AG. (2013). Tibialis anterior muscle fascicle dynamics adequately
576 represent postural sway during standing balance. *J Appl Physiol (1985)* **115,** 1742-1750.

577
578 De Luca CJ. (1985). Control properties of motor units. *J Exp Biol* **115,** 125-136.

579
580 De Luca CJ & Erim Z. (1994). Common drive of motor units in regulation of muscle force. *Trends Neurosci*
581 **17,** 299-305.

582
583 Del Vecchio A, Casolo A, Negro F, Scorcelletti M, Bazzucchi I, Enoka R, Felici F & Farina D. (2019). The
584 increase in muscle force after 4 weeks of strength training is mediated by adaptations in motor
585 unit recruitment and rate coding. *J Physiol* **597,** 1873-1887.

586
587 Del Vecchio A, Ubeda A, Sartori M, Azorin JM, Felici F & Farina D. (2018). Central nervous system
588 modulates the neuromechanical delay in a broad range for the control of muscle force. *J Appl*
589 *Physiol (1985)* **125,** 1404-1410.

590
591 Dideriksen JL & Farina D. (2019). Amplitude cancellation influences the association between frequency
592 components in the neural drive to muscle and the rectified EMG signal. *PLoS Comput Biol* **15,**
593 e1006985.

594
595 Dideriksen JL, Negro F, Falla D, Kristensen SR, Mrachacz-Kersting N & Farina D. (2018). Coherence of the
596 Surface EMG and Common Synaptic Input to Motor Neurons. *Front Hum Neurosci* **12,** 207.

597
598 Dieterich AV, Botter A, Vieira TM, Peolsson A, Petzke F, Davey P & Falla D. (2017). Spatial variation and
599 inconsistency between estimates of onset of muscle activation from EMG and ultrasound. *Sci Rep*
600 **7,** 42011.

601
602 Enoka RM. (2004). Biomechanics and neuroscience: a failure to communicate. *Exerc Sport Sci Rev* **32,** 1-3.

603
604 Farina D, Cescon C & Merletti R. (2002). Influence of anatomical, physical, and detection-system
605 parameters on surface EMG. *Biol Cybern* **86,** 445-456.

606
607 Farina D & Negro F. (2015). Common synaptic input to motor neurons, motor unit synchronization, and
608 force control. *Exerc Sport Sci Rev* **43,** 23-33.

609
610 Farina D, Negro F, Gazzoni M & Enoka RM. (2008). Detecting the unique representation of motor-unit
611 action potentials in the surface electromyogram. *J Neurophysiol* **100,** 1223-1233.

612
613 Farina D, Negro F, Muceli S & Enoka RM. (2016). Principles of Motor Unit Physiology Evolve With Advances
614 in Technology. *Physiology (Bethesda)* **31,** 83-94.

615
616 Farris DJ & Lichtwark GA. (2016). UltraTrack: Software for semi-automated tracking of muscle fascicles in
617 sequences of B-mode ultrasound images. *Comput Methods Programs Biomed* **128,** 111-118.

618
619 Gillett JG, Barrett RS & Lichtwark GA. (2013). Reliability and accuracy of an automated tracking algorithm
620 to measure controlled passive and active muscle fascicle length changes from ultrasound. *Comput*
621 *Methods Biomech Biomed Engin* **16,** 678-687.

622
623 Glaser V & Holobar A. (2019). Motor Unit Identification From High-Density Surface Electromyograms in
624 Repeated Dynamic Muscle Contractions. *IEEE Trans Neural Syst Rehabil Eng* **27,** 66-75.

625
626 Heintz S & Gutierrez-Farewik EM. (2007). Static optimization of muscle forces during gait in comparison
627 to EMG-to-force processing approach. *Gait Posture* **26,** 279-288.

628
629 Hodges PW, Pengel LH, Herbert RD & Gandevia SC. (2003). Measurement of muscle contraction with
630 ultrasound imaging. *Muscle Nerve* **27,** 682-692.

631
632 Holobar A & Farina D. (2014). Blind source identification from the multichannel surface electromyogram.
633 *Physiol Meas* **35,** R143-165.

634
635 Hug F, Lacourpaille L & Nordez A. (2011). Electromechanical delay measured during a voluntary
636 contraction should be interpreted with caution. *Muscle Nerve* **44,** 838-839.

637
638 Lauber B, Lichtwark GA & Cresswell AG. (2014). Reciprocal activation of gastrocnemius and soleus motor
639 units is associated with fascicle length change during knee flexion. *Physiol Rep* **2**.

640
641 Lichtwark GA & Wilson AM. (2007). Is Achilles tendon compliance optimised for maximum muscle
642 efficiency during locomotion? *J Biomech* **40,** 1768-1775.

643
644 Ling YT, Ma CZ, Shea QTK & Zheng YP. (2020). Sonomechanomyography (SMMG): Mapping of Skeletal
645 Muscle Motion Onset during Contraction Using Ultrafast Ultrasound Imaging and Multiple Motion
646 Sensors. *Sensors (Basel)* **20**.

647
648 Marsh E, Sale D, McComas AJ & Quinlan J. (1981). Influence of joint position on ankle dorsiflexion in
649 humans. *J Appl Physiol Respir Environ Exerc Physiol* **51,** 160-167.

650
651 Martinez-Valdes E, Falla D, Negro F, Mayer F & Farina D. (2017a). Differential Motor Unit Changes after
652 Endurance or High-Intensity Interval Training. *Med Sci Sports Exerc* **49,** 1126-1136.

653

654 Martinez-Valdes E, Negro F, Falla D, Dideriksen JL, Heckman CJ & Farina D. (2020a). Inability to increase
655 the neural drive to muscle is associated with task failure during submaximal contractions. *J*
656 *Neurophysiol* **124,** 1110-1121.

657
658 Martinez-Valdes E, Negro F, Farina D & Falla D. (2020b). Divergent response of low- versus high-threshold
659 motor units to experimental muscle pain. *J Physiol* **598,** 2093-2108.

660
661 Martinez-Valdes E, Negro F, Laine CM, Falla D, Mayer F & Farina D. (2017b). Tracking motor units
662 longitudinally across experimental sessions with high-density surface electromyography. *J Physiol*
663 **595,** 1479-1496.

664
665 Mayfield DL, Cresswell AG & Lichtwark GA. (2016). Effects of series elastic compliance on muscle force
666 summation and the rate of force rise. *J Exp Biol* **219,** 3261-3270.

667
668 Murphy S, Durand M, Negro F, Farina D, Hunter S, Schmit B, Gutterman D & Hyngstrom A. (2019). The
669 Relationship Between Blood Flow and Motor Unit Firing Rates in Response to Fatiguing Exercise
670 Post-stroke. *Front Physiol* **10,** 545.

671
672 Negro F, Holobar A & Farina D. (2009). Fluctuations in isometric muscle force can be described by one
673 linear projection of low-frequency components of motor unit discharge rates. *J Physiol* **587,** 5925-
674 5938.

675
676 Negro F, Muceli S, Castronovo AM, Holobar A & Farina D. (2016). Multi-channel intramuscular and surface
677 EMG decomposition by convolutive blind source separation. *J Neural Eng* **13,** 026027.

678
679 Oliveira AS & Negro F. (2021). Neural Control of Matched Motor Units during Muscle Shortening and
680 Lengthening at Increasing Velocities. *J Appl Physiol (1985)*.

681
682 Pasquet B, Carpentier A & Duchateau J. (2005). Change in muscle fascicle length influences the
683 recruitment and discharge rate of motor units during isometric contractions. *J Neurophysiol* **94,**
684 3126-3133.

685
686 Pasquet B, Carpentier A & Duchateau J. (2006). Specific modulation of motor unit discharge for a similar
687 change in fascicle length during shortening and lengthening contractions in humans. *J Physiol* **577,**
688 753-765.

689
690 Pincheira PA, Hoffman BW, Cresswell AG, Carroll TJ, Brown NAT & Lichtwark GA. (2018). The repeated
691 bout effect can occur without mechanical and neuromuscular changes after a bout of eccentric
692 exercise. *Scand J Med Sci Sports* **28,** 2123-2134.

693

694 Raiteri BJ, Cresswell AG & Lichtwark GA. (2018). Muscle-tendon length and force affect human tibialis
695 anterior central aponeurosis stiffness in vivo. *Proc Natl Acad Sci U S A* **115,** E3097-E3105.

696
697 Reeves ND & Narici MV. (2003). Behavior of human muscle fascicles during shortening and lengthening
698 contractions in vivo. *J Appl Physiol (1985)* **95,** 1090-1096.

699
700 Romaiguere P, Vedel JP & Pagni S. (1993). Comparison of fluctuations of motor unit recruitment and de-
701 recruitment thresholds in man. *Exp Brain Res* **95,** 517-522.

702
703 Son J, Hwang S & Kim Y. (2010). An EMG-based muscle force monitoring system. *Journal of Mechanical*
704 *Science and Technology* **24,** 2099-2105.

705
706 Stephens JA, Reinking RM & Stuart DG. (1975). The motor units of cat medial gastrocnemius: electrical
707 and mechanical properties as a function of muscle length. *J Morphol* **146,** 495-512.

708
709 Suzuki R, Kanehisa H, Washino S, Watanabe H, Shinohara M & Yoshitake Y. (2021). Reconstruction of net
710 force fluctuations from surface EMGs of multiple muscles in steady isometric plantarflexion. *Exp*
711 *Brain Res* **239,** 601-612.

712
713 Thompson CK, Negro F, Johnson MD, Holmes MR, McPherson LM, Powers RK, Farina D & Heckman CJ.
714 (2018). Robust and accurate decoding of motoneuron behaviour and prediction of the resulting
715 force output. *J Physiol* **596,** 2643-2659.

716
717 Tytell ED, Holmes P & Cohen AH. (2011). Spikes alone do not behavior make: why neuroscience needs
718 biomechanics. *Curr Opin Neurobiol* **21,** 816-822.

719
720 Vieira TM & Botter A. (2021). The Accurate Assessment of Muscle Excitation Requires the Detection of
721 Multiple Surface Electromyograms. *Exerc Sport Sci Rev* **49,** 23-34.

722
723 Yavuz US, Negro F, Falla D & Farina D. (2015). Experimental muscle pain increases variability of neural
724 drive to muscle and decreases motor unit coherence in tremor frequency band. *J Neurophysiol*
725 **114,** 1041-1047.

726
727 Yoshitake Y & Shinohara M. (2013). Low-frequency component of rectified EMG is temporally correlated
728 with force and instantaneous rate of force fluctuations during steady contractions. *Muscle Nerve*
729 **47,** 577-584.

730

731

732

FIGURE LEGENDS

Figure 1. Study schematic. MVC, maximum voluntary contraction torque.

Figure 2. High-density surface electromyography (HDEMG) ultrasound-transparent electrodes. A) Back (up) and front (down) of the 32-channel (10 mm inter-electrode distance) electrode grid. B) HDEMG electrode grid with 32-channel HDEMG amplifier (connected on top of the electrode) and flat ultrasound probe can be seen on the left. Ultrasound image of proximal tibialis anterior muscle can be seen on the right. Note the quality of the image with accurate visualization of fascicles and, superficial, intermediate and deep aponeuroses.

Figure 3. Motor unit identification during isometric contractions. A total of 11 motor units (MUs) were decomposed from the HDEMG signals in a representative participant during an isometric contraction at 20% of the maximum voluntary torque (0° of plantarflexion). Instantaneous firing rate with torque profile can be seen on the left of the figure while 2D motor unit action potentials (MUAPs) from each of these motor units can be seen on the right of the figure. Note the clear differences in MUAP shape for each of the identified units.

Figure 4. Motor unit tracking. A representative example of a motor unit that was tracked across two-plantarflexion angles at 20% MVC can be seen on the figure. For this motor unit, the action potentials (single differential) had a cross correlation coefficient of 0.90 across angles. The instantaneous firing rate of this unit can be seen on the bottom of the figure.

Figure 5. Fascicle length tracking procedure and correlation with torque and motor unit data. A) A tibialis anterior ultrasound image and a fascicle of interest (red) can be seen on top of the figure. The length data obtained from the tracking of this fascicle was then correlated with torque and cumulative spike train (CST) signals (bottom). Fascicle length data is presented as the amount

of shortening from rest to target torque (fascicle length during rest-fascicle length reached at target torque). Note that fascicle shortening precedes the generation of torque during the ramp-up phase of the contraction and then returns to baseline values after the torque signal returns to zero. B) Common fluctuations from the three generated signals (torque, CST and fascicle length) in the steady-torque part of the contraction can be seen on top of the figure. Cross-correlation and lag (delay, ms) results between CST vs torque, CST vs fascicle length (fascicle) and fascicle vs torque can be seen on the bottom of the figure.

Figure 6. Cross-correlation lag (delay) results during sustained and sinusoidal isometric contractions. Delays between cumulative spike train (CST) vs torque, CST vs fascicle length (fascicle) and fascicle vs torque can be seen for sustained (A) and sinusoidal (B) isometric contractions at 0° and 30° of plantarflexion at 20% MVC and 40% MVC. *, significant effect of joint angle ($p<0.05$).

Figure 7. Recruitment and de-recruitment thresholds in relation to torque and fascicle length. A representative example of recruitment and de-recruitment threshold of a motor unit in relation to torque and fascicle length can be seen on the left of the figure. The recruitment threshold for this unit was higher than the de-recruitment threshold when calculated as %MVC torque (green dashed line) but similar when calculated as fascicle shortening length (blue dashed line). Fascicle length data is presented as the amount of shortening from rest to target torque (fascicle length during rest-fascicle length reached at target torque). The same results can be appreciated by the group of participants on the right of the figure as recruitment thresholds are consistently higher than de-recruitment thresholds across target torques and angles when considered as %MVC torque (upper right) but similar when calculated from fascicle length data (lower right). *,

777 significant effect of recruitment-de-recruitment ($p<0.05$). #, significant effect of joint angle
778 ($p<0.05$). Ψ, significant effect of torque ($p<0.05$).

779

780 **ADDITIONAL INFORMATION SECTION**

781 Author contributions

782 Experiments were performed at the School of Human Movement and Nutrition Sciences,
783 University of Queensland, Queensland, Australia. E.M.-V. designed research; E.M.-V and P.P.
784 performed experiments; E.M.-V. and F.N. analysed the data; E.M.-V., F.N., A.B., G.C., D.F., P.P.,
785 G.L. and A.C. interpreted the data and contributed to the drafting of the article. All authors have
786 read and approved final submission. All authors agree to be accountable for all aspects of the
787 work, ensuring that questions related to the accuracy or integrity of any part are appropriately
788 investigated and resolved. All persons designated as authors qualify for authorship, and all those
789 who qualify for authorship are listed.

790 Competing interests

791 All authors declare no conflict of interest.

792 Funding

793 This study was partially funded with the University of Birmingham International Engagement Fund (BIEF)
794 awarded to E.M.-V.

795

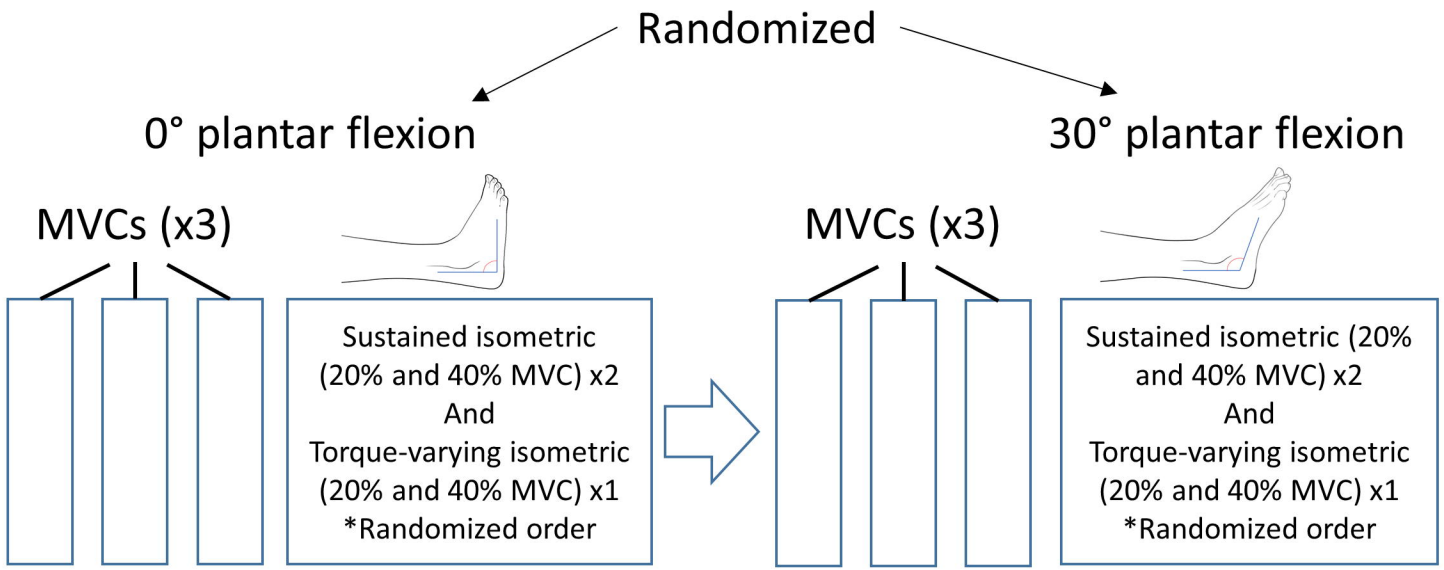
Randomized
0° plantar flexion
30° plantar flexion
MVCs (x3)
MVCs (x3)
Sustained isometric (20% and 40% MVC) x2
And
Torque-varying isometric (20% and 40% MVC) x1
*Randomized order
Sustained isometric (20% and 40% MVC) x2
And
Torque-varying isometric (20% and 40% MVC) x1
*Randomized order

A)

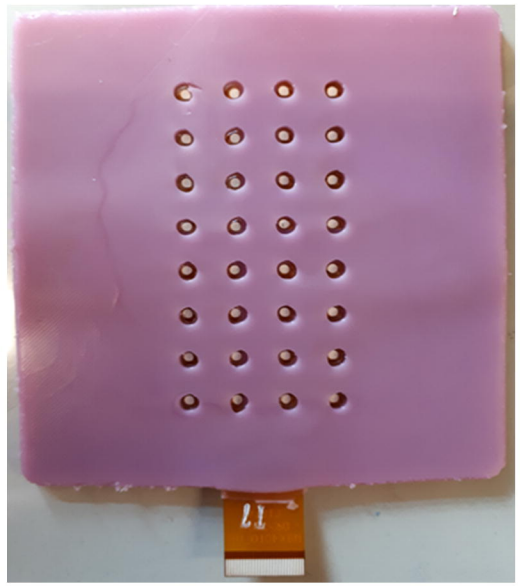

B)

Distal Proximal

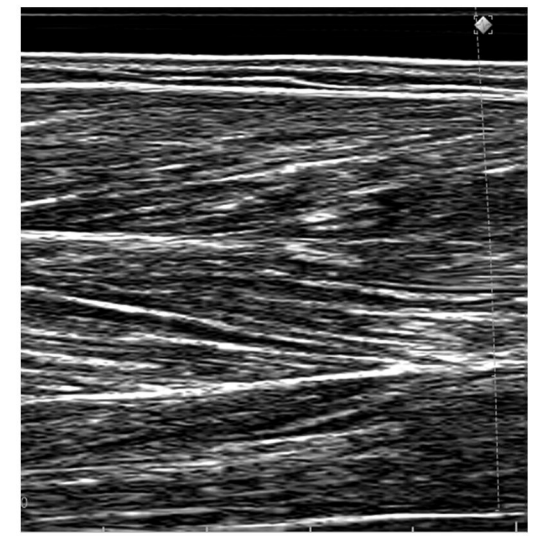

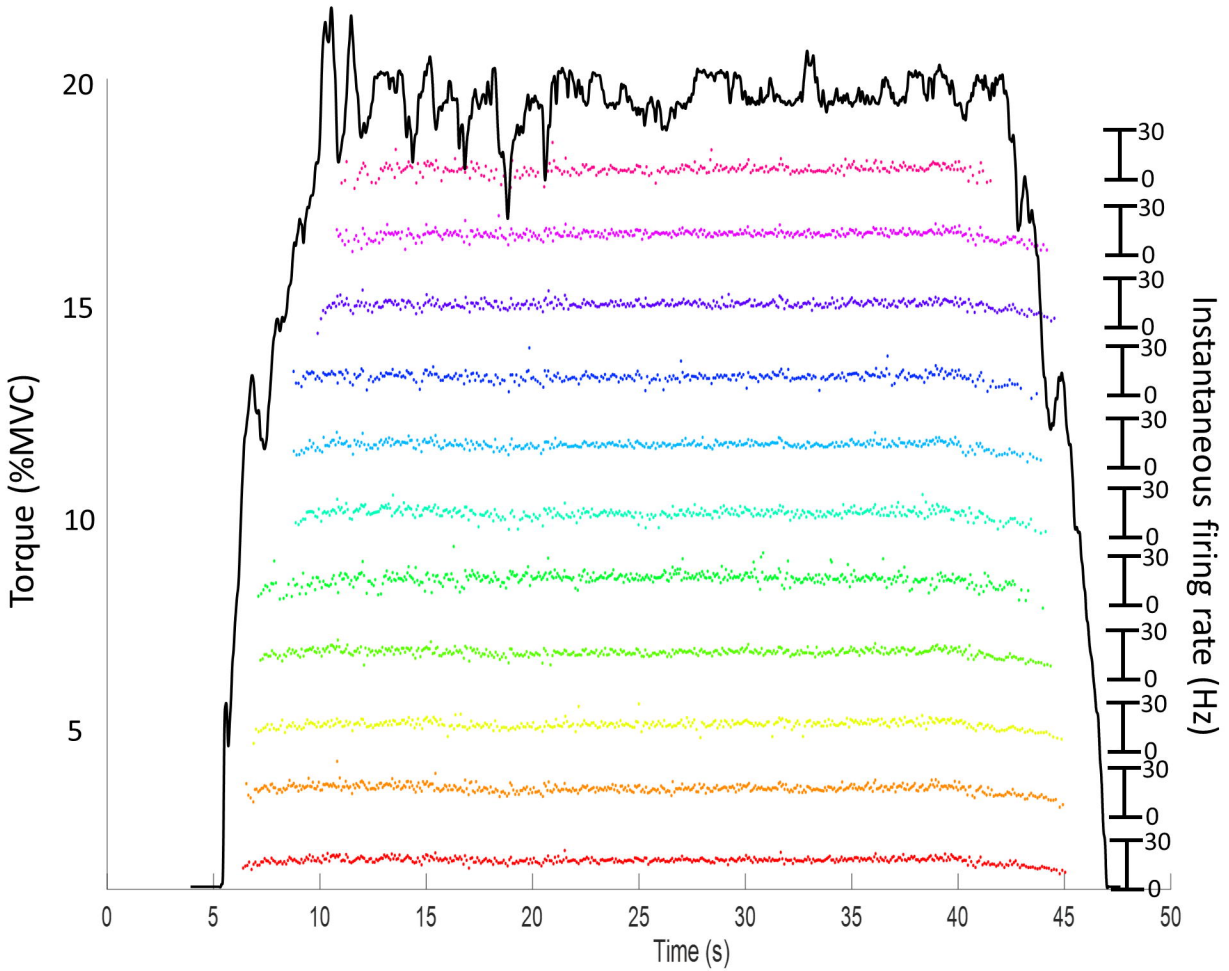
Torque (%MVC)
20
15
10
5
0
5
10
15
20
25
30
35
40
45
50
Time (s)
Instantaneous firing rate (Hz)
30
0

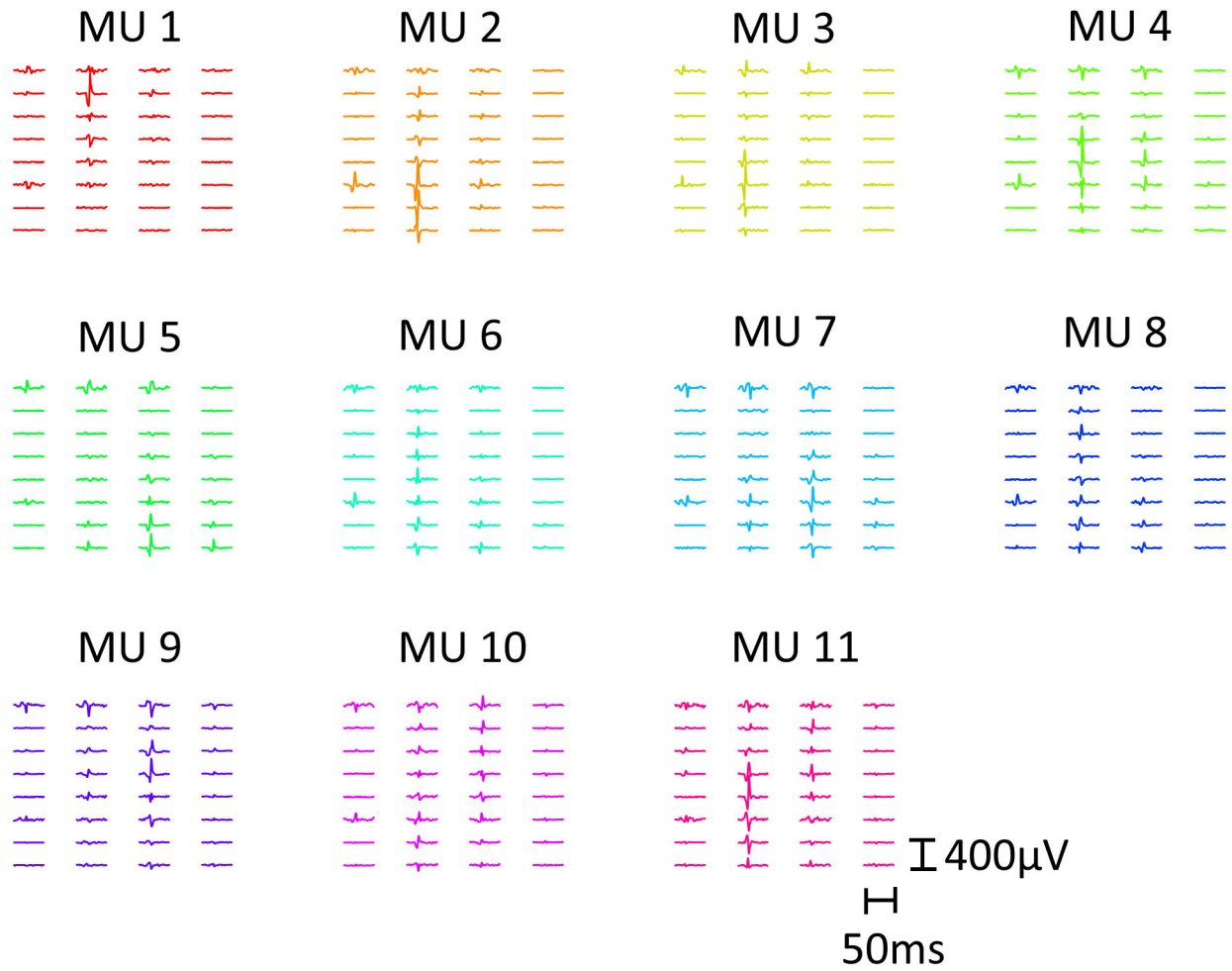
MU 1
MU 2
MU 3
MU 4
MU 5
MU 6
MU 7
MU 8
MU 9
MU 10
MU 11
400µV
50ms

Cross correlation = 0.90

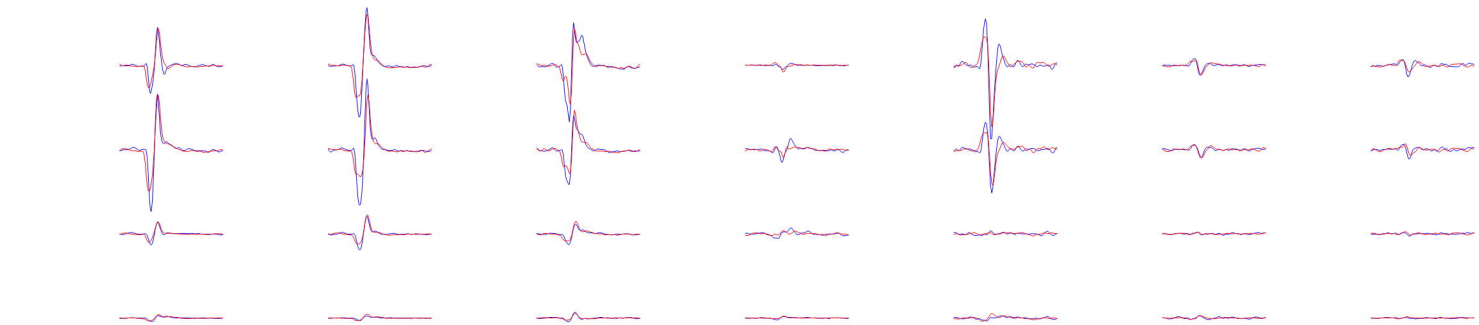

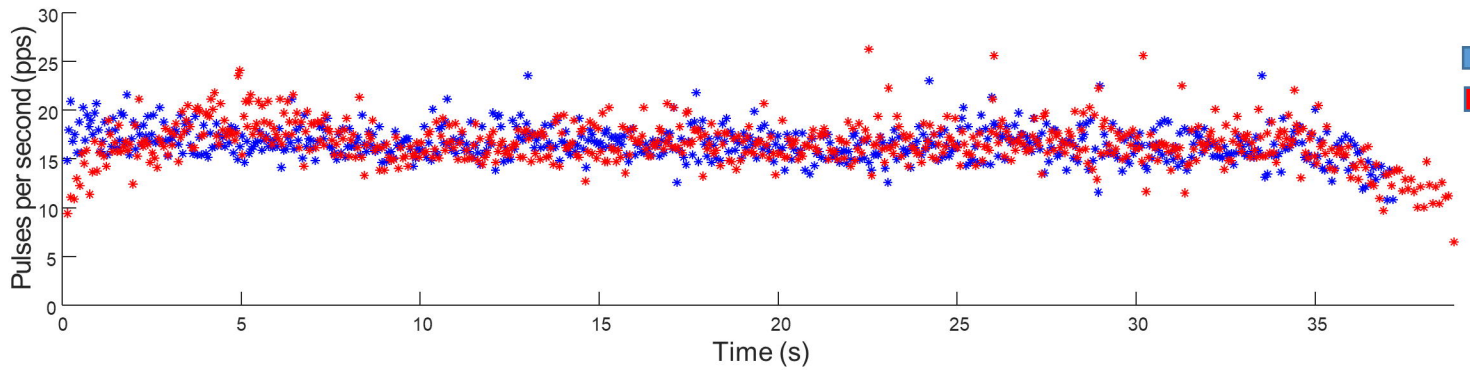

0˚ plantar flexion
30˚ plantar flexion

A)

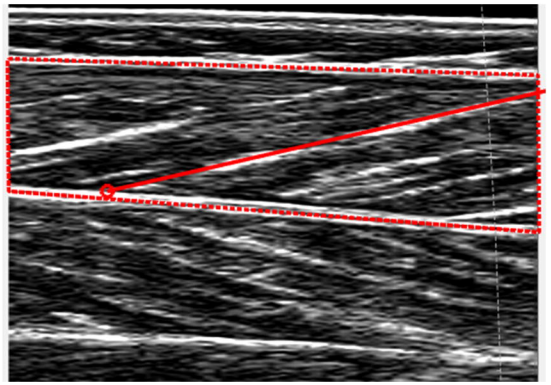

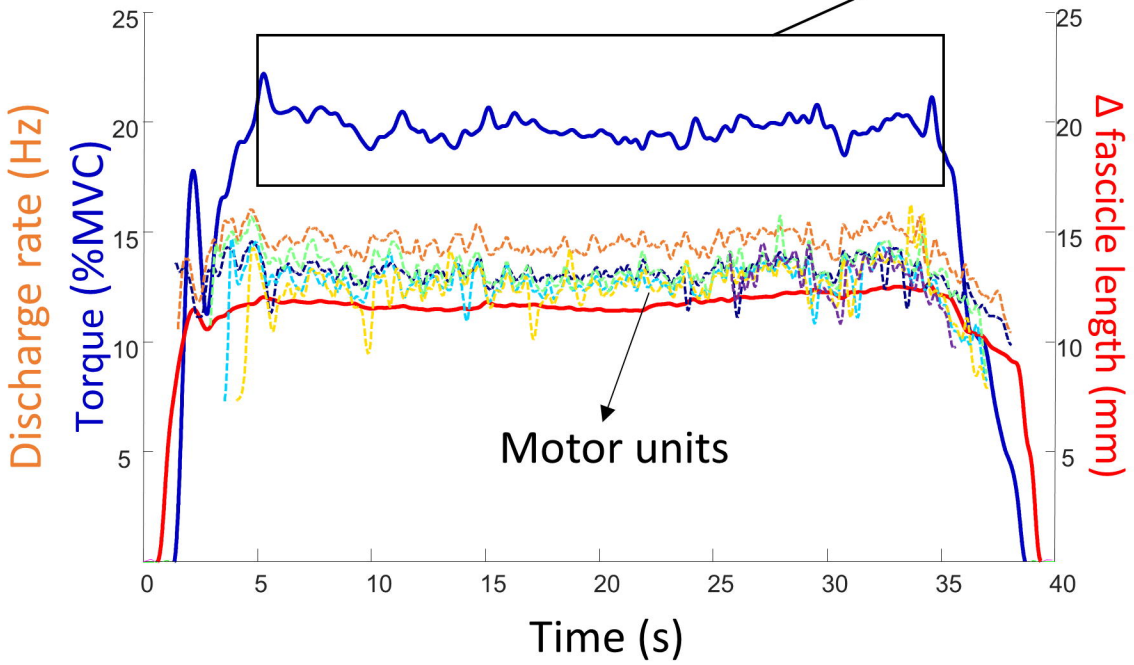

B)

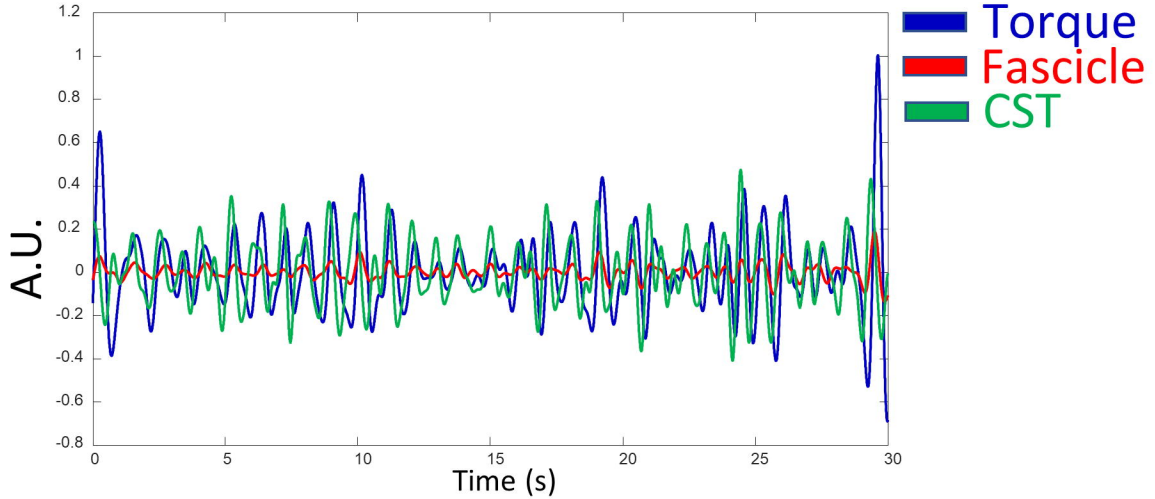

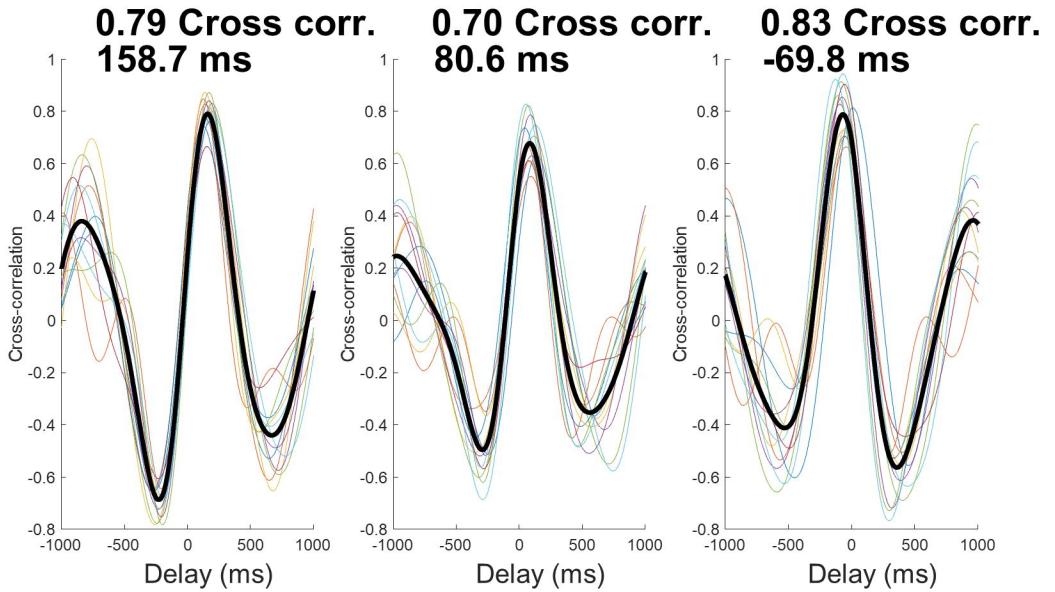

CST vs TORQUE CST vs FASCICLE TORQUE vs FASCICLE

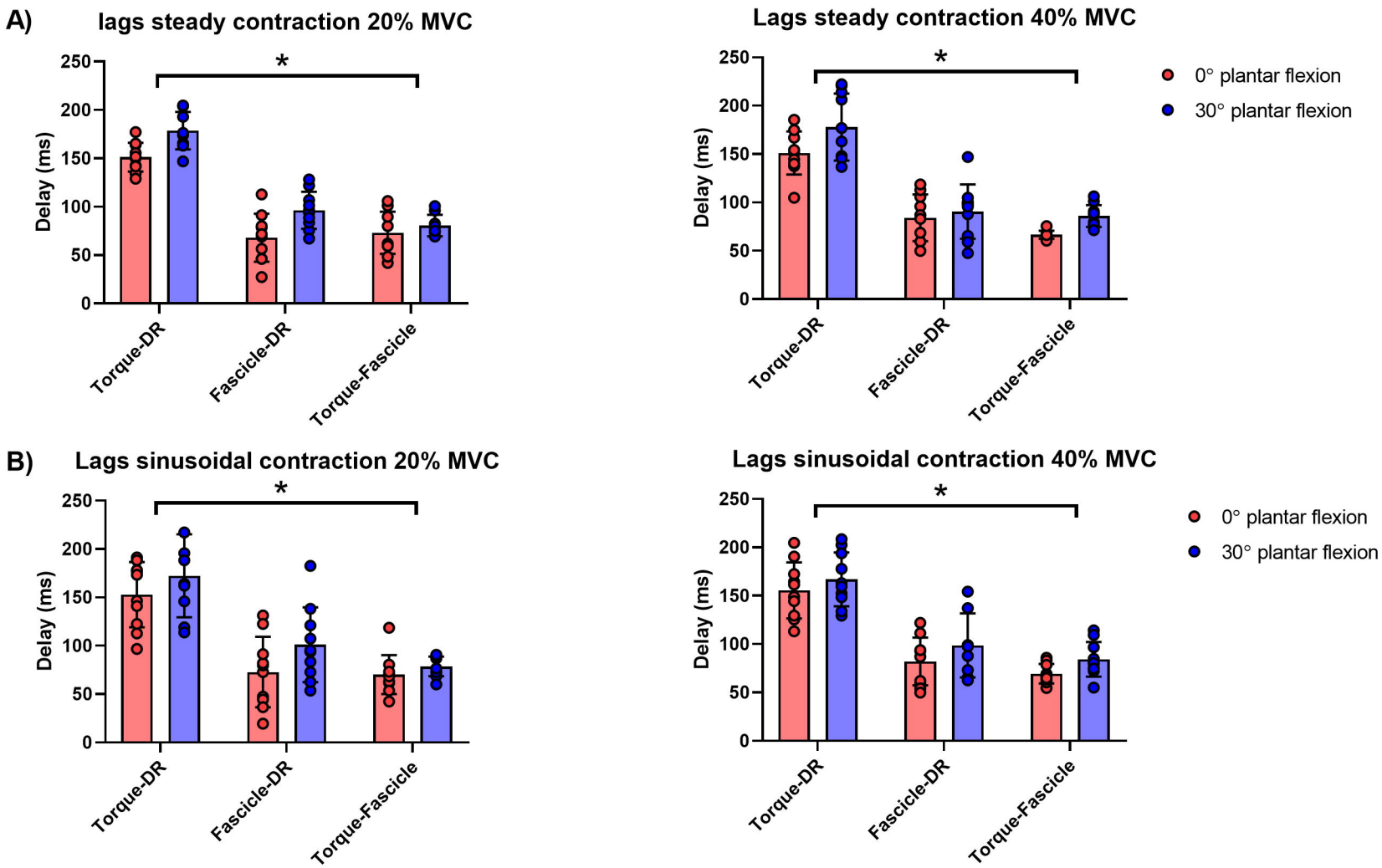
A)
lags steady contraction 20% MVC
Lags steady contraction 40% MVC
B)
Lags sinusoidal contraction 20% MVC
Lags sinusoidal contraction 40% MVC
Delay (ms)
250
200
150
100
50
0
*
Torque-DR
Fascicle-DR
Torque-Fascicle
0° plantar flexion
30° plantar flexion

A)

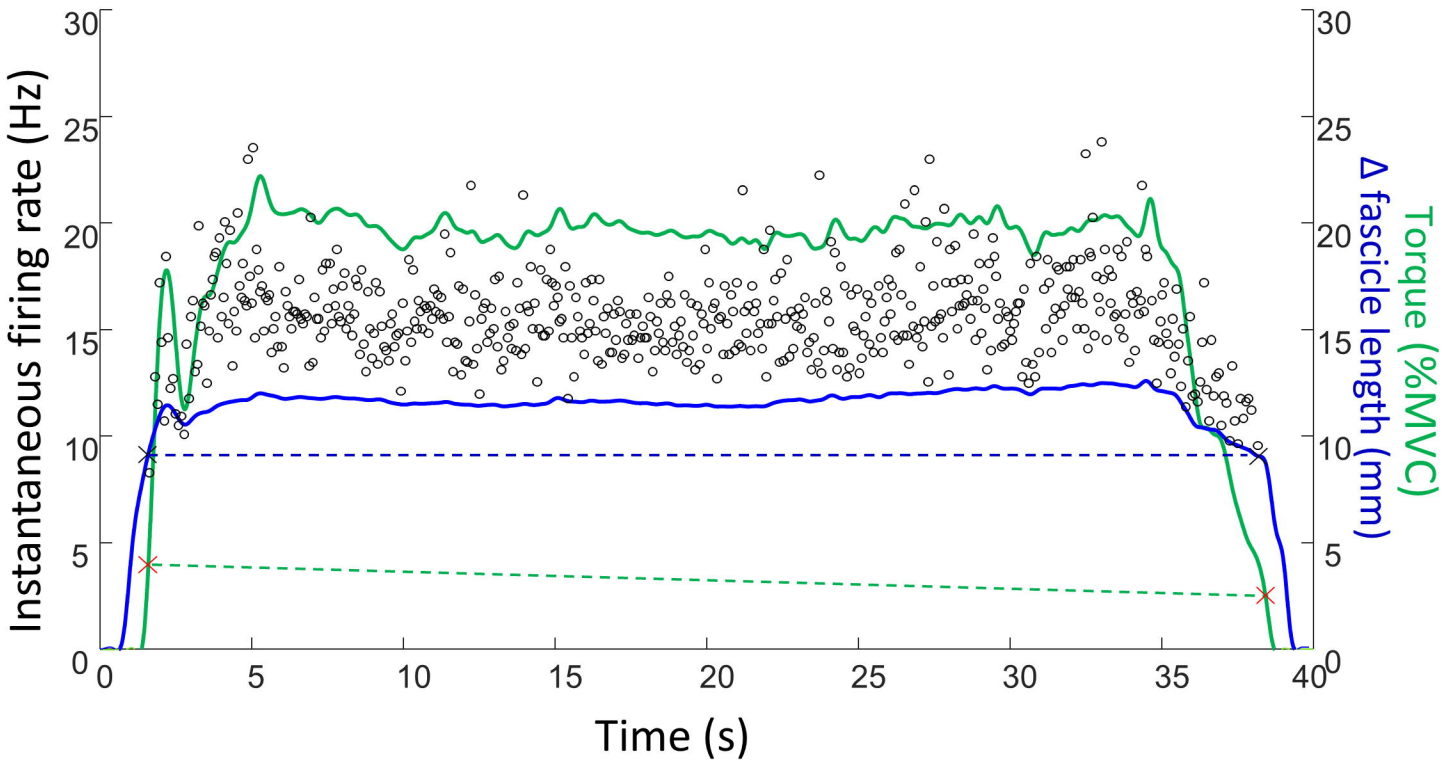
Instantaneous firing rate (Hz)
Torque (%MVC)
Δ fascicle length (mm)
Time (s)
0
5
10
15
20
25
30
35
40

B)

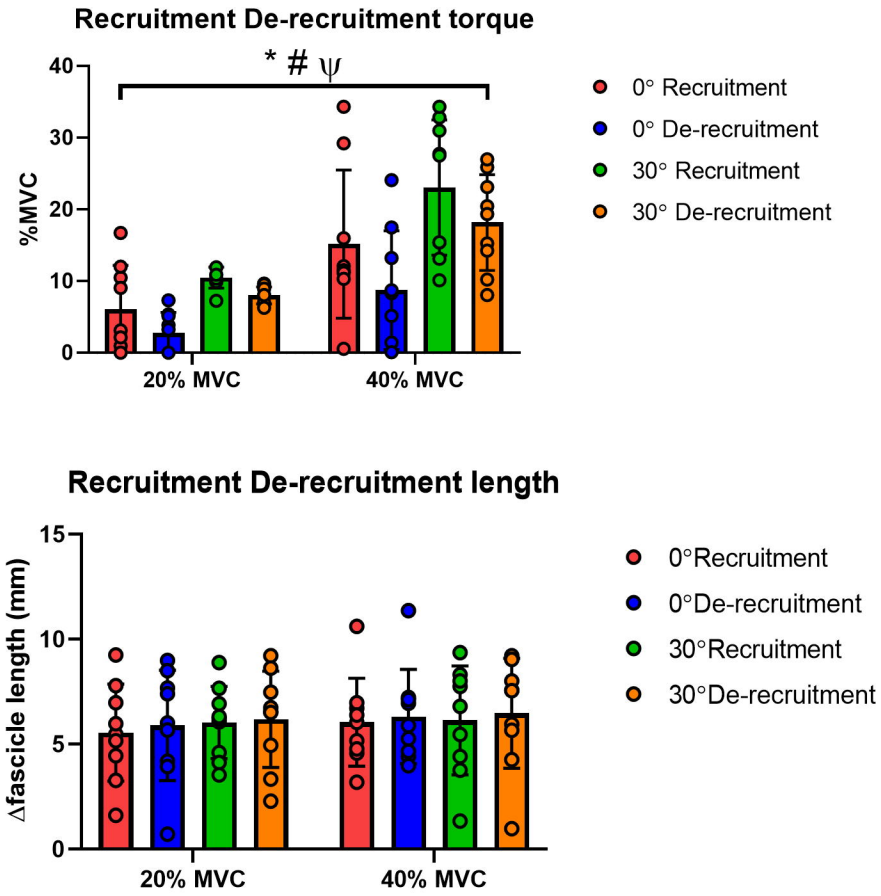
Recruitment De-recruitment torque
* # ψ
%MVC
20% MVC
40% MVC
0° Recruitment
0° De-recruitment
30° Recruitment
30° De-recruitment
Recruitment De-recruitment length
Δfascicle length (mm)
20% MVC
40% MVC
0°Recruitment
0°De-recruitment
30°Recruitment
30°De-recruitment